

Human detectors are surprisingly powerful reward models

Kumar Ashutosh^{1,2} XuDong Wang¹ Xi Yin¹ Kristen Grauman²
Adam Polyak¹ Ishan Misra¹ Rohit Girdhar¹
¹Meta AI ²University of Texas at Austin

<https://huda-reward-model.github.io/>

Abstract

Video generation models have recently achieved impressive visual fidelity and temporal coherence. Yet, they continue to struggle with complex, non-rigid motions, especially when synthesizing humans performing dynamic actions such as sports, dance, etc. Generated videos often exhibit missing or extra limbs, distorted poses, or physically implausible actions. In this work, we propose a remarkably simple reward model, HUDA, to quantify and improve the human motion in generated videos. HUDA integrates human detection confidence for appearance quality, and a temporal prompt alignment score to capture motion realism. We show this simple reward function that leverages off-the-shelf models without any additional training, outperforms specialized models finetuned with manually annotated data. Using HUDA for Group Reward Policy Optimization (GRPO) post-training of video models, we significantly enhance video generation, especially when generating complex human motions, outperforming state-of-the-art models like Wan 2.1, with win-rate of 73%. Finally, we demonstrate that HUDA improves generation quality beyond just humans, for instance, significantly improving generation of animal videos and human-object interactions.

1. Introduction

Text to video generation is an active area of research with growing applications across the industry, including in education, film-making, marketing, and social media. From an educational app to help one master their gymnastic moves, to a fun social media trend showing one perform parkour, there is a particular emphasis on generating high fidelity videos of humans. Despite impressive progress in the past few years, the generations do not always satisfy the desired requirements. While recent work has developed measures to quantify and fix inaccuracies across some axes like prompt faithfulness or overall quality, it has been very challenging to generate accurate human shape and motion, especially when the human is performing complex actions

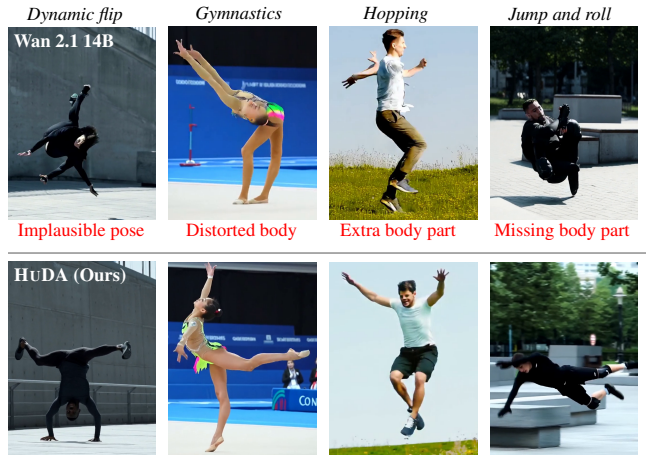


Figure 1. **HUDA** is a reward model to quantify the human appearance and motions in generated videos. HUDA detects extra or missing body parts, implausible body pose, and misalignment with the prompt. Training a video diffusion model with HUDA using GRPO results in improved human appearance and motion in generated videos (bottom) compared to state-of-the-art baseline (top). Videos corresponding to all figures in the paper are provided in the Appendix A.

(cf. Fig. 1 (top)). This is true even for advanced proprietary models such as SORA-2 and VEO-3 (cf. Fig. 2).

In this work, we aim to address this challenging task of assessing and generating videos with complex human actions. We propose a remarkably simple reward function to assess the quality of generations, **HUDA**: that leverages **H**uman Detection and temporal prompt **A**lignment. We find that the frame-level object detection [24] confidence score for the ‘human’ class is a strong indicator of how realistic the human in the generated video is. By itself, however, this reward is easy to hack—a low-motion video containing the “simpler” part of the action can obtain a perfect score by generating the human poses perfectly. For example, a video showing only the takeoff phase of the backflip, before the person flips in mid-air, the latter of which is typically harder for models to generate. To counteract this, we strengthen the motion assessment by decomposing the

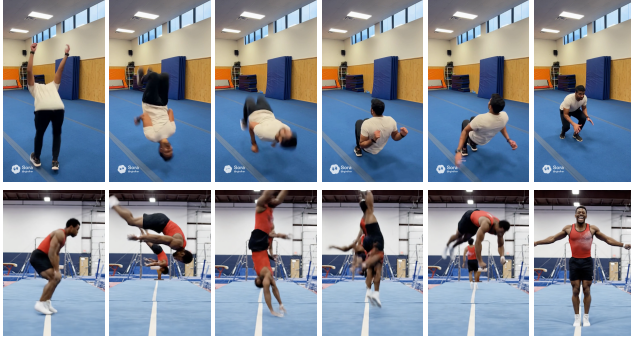


Figure 2. **SORA-2 and Veo-3 generations** for the prompts “@rgirdhar (author) doing a backflip,” and “A person doing a backflip in a gym.” Even state-of-the-art proprietary models struggle to generate complex human actions. Full video in Appendix A.

input text prompt into “phase captions” corresponding to different phases of an action, and evaluating the similarity of these captions with uniformly sampled frames. Finally, we aggregate frame-level confidences for both models into a video-level reward score.

The critical challenge in designing a reward model to evaluate the realism of generated human actions is to understand and quantify all the failure cases, including extra or missing body parts, implausible body pose like knee bending forward, and implausible movements like a very high jump or a sliding effect without any force. Using a video language model (VLM) [36] is not enough, as we also show in our experiments. There are prior works in identifying invalid human generations—missing or redundant body parts [42], or incorrect physics [32]. There are also efforts to solve this problem in a data-driven way by annotating a large amount of images if they have an anomaly [8, 42, 47], and training models on that. HUDA, on the other hand, is a much simpler approach that does not require any training, and leverages off-the-shelf computer vision models in a zero-shot manner to build a powerful reward function.

Being able to evaluate the correctness of human motion and appearance also enables *post-training* video diffusion models with HUDA as a reward model using reinforcement learning techniques such as Direct Preference Optimization (DPO) [27, 37] or Group Reward Policy Optimization (GRPO) [26, 45]. This idea was also recently used to improve visual and motion quality, and prompt faithfulness of video models [26, 27, 37, 45]. We use HUDA to tune video diffusion models using GRPO to improve complex human action generation. We experiment with state-of-the-art models such as Wan 2.1 [38] 1.3B and 14B variants, although our approach is applicable to any video diffusion model. For evaluation, we use a human preference study to first establish that our reward model strongly correlates with human judgement, compared to all the prior works. Next, we conduct another set of human preference studies

to establish the improvements in the human appearance and motion in the generated videos using HUDA. We show significant improvements over already strong models like Wan 2.1 14B, with win-rate of 73%, setting a new state-of-the-art in video generation for complex human actions. Finally, we show that the training guides the model to better understand general bodily deformations, thus leading to improvements in animal video generations and human object interactions, without any specific training or optimization.

2. Related Work

Video generation. Research in video generation aims to generate a video, given a text prompt, or other conditioning signals like an image or a short video. Traditional approaches use GAN [41, 46], pixel-level regression [9, 19], and other variational/stochastic models [6, 13, 22]. Recent advances in video diffusion models [1, 3, 11, 12, 15–18, 20, 21, 34, 38, 40, 48] have enabled high-quality, realistic generations. Current methods are able to generate videos that are true to the conditioning signal, while still ensuring diversity with different starting input noise.

Despite the impressive progress, diffusion models are typically trained only using a simple L2 loss, and do not have additional visual, motion, human appearance objectives. Consequently, the outputs are not optimized on all crucial axes—text faithfulness, visual quality, and importantly, human appearance and actions. Prior works also observe these shortcomings of video diffusion models [26, 27, 45]. While most of these observations result in improvement along visual quality and prompt faithfulness, we design a novel training setup to train a text-to-video diffusion model to generate videos with correct human appearance without abnormalities.

Generating videos of people. Prior works acknowledge issues with human appearance in images and videos [8, 32, 42, 47, 49]. FHAD [42], HumanRefiner [8], and HEIE [47] are manually annotated datasets containing real and generated images, with the label of whether the shown human is realistic or not. These datasets are then used to train models that can score the correctness of human appearance in generated images and videos [8, 42, 49]. Alternatively, FinePhys [32] incorporates physics learned from gymnasium videos to improve in-domain video generation with more realistic gymnasium sequences. HumanDreamer [39] decouples the video generation problem to text-to-pose and pose-to-video generation, while manually annotating the pose representation for noise-free two-stage training. Finally, HEIE [47] proposes a chain-of-thought (CoT) multi-modal large language model (MLLM) to determine whether the generated image contains implausible human poses, relying on human annotated data.

In contrast to prior work, we propose a novel simple reward model that can score the plausibility of a human in

the generated video. We do not make any assumption about the task the person is doing, unlike [32], and is zero-shot, unlike [8, 39, 42, 47, 49]. We also do not focus solely on data-driven physical parameter estimation, as in [32], keeping our approach generalizable. We further show the effectiveness of the reward model by using it to post-train video diffusion models with GRPO to generate realistic human appearance and movement.

Diffusion model post-training. Training a diffusion model from scratch to optimize on certain axes is computationally expensive. Rather, recent methods use *post-training* approaches to align the generated image or video outputs towards the desired behavior [26, 27, 37, 45]. Several reinforcement learning (RL) approaches are used depending on the setup. Direct preference optimization (DPO) directly optimizes model outputs against preference pairs, eliminating the need for an explicit reward model and policy optimization stage [5, 27, 30, 37]. Typically, the preference pairs are obtained via human annotations, but can also be obtained using a reward model [27]. On the other hand, group relative policy optimization (GRPO) uses an explicit reward model to update the diffusion model policy [26, 45]. In this work, we prefer GRPO over DPO for its on-policy training, the use of continuous richer reward signal, and the ability to use a multi-objective reward.

3. Method

In this section, we first formally describe the problem statement, followed by our proposed approach.

3.1. Problem definition

Given videos \mathbf{V}_1 and \mathbf{V}_2 , we aim to design a reward function, R , such that $R(\mathbf{V}_1) > R(\mathbf{V}_2)$ iff \mathbf{V}_1 has better human appearance and motion, compared to \mathbf{V}_2 , while portraying the same action. In particular, the characteristics of a good human appearance and motion include no extra or missing body part, no abnormal body pose, and no abnormal body movement. In other words, any cue that allows a viewer to classify the video as implausible based on the human in the video should result in a lower value of the function R . Our choice of R is a superset of the considerations in prior work, which only focuses on missing and extra body parts [42], or incorrect physics [32]. In addition to designing R , we aim to improve video generation performance by using R in a reinforcement learning pipeline as a reward model. In particular, we show improvement in text-to-video (T2V) generations by using R in GRPO. While our focus in this work is T2V, our approach is general and can be easily extended to other video generations tasks such as image-to-video (I2V) or video editing (V2V).

3.2. Proposed reward model R

We propose HUDA: a simple linear combination of a) **Human Detection** score, and b) temporal prompt **Alignment**. As we show in experiments later, this simple function combining off-the-shelf models captures human motion and appearance quality better than even approaches trained for this task. We now describe the components of this reward function, followed by how we use it for improving video generation in RL post-training.

Human detection score (H-score) measures the quality of humans in all the frames, and it is low if there are missing or extra body parts, implausible body pose, and incorrect physics. We measure the implausibility per frame, and then aggregate the scores into a video-level appearance quality.

Given an object detector model $\mathcal{D} : \mathbb{R}^{H \times W \times 3} \rightarrow \mathcal{O}$ (e.g., [10, 14, 24]), where \mathcal{O} is the object name or the corresponding class, we quantify the detection score of \mathbf{V} as

$$\min_{\forall t} \left[\sum_{\tau=t}^{t+W} \max_{\forall B} \{ \mathbb{P}(\mathcal{D}(\mathbf{V}_\tau[B]) = \text{human}) \} \right],$$

where W is the window size, B is any bounding box in the frame \mathbf{V}_t , and \mathbb{P} refers to the probability of that detection. Concisely, the human detection score is the minimum confidence score over all fixed-size windows, where a window’s confidence score is the sum of highest likelihood of the object detector predicting a human in the frame, for all frames in that window. We use minimum over average/max aggregation to capture the worst human appearance in a video. Note that this scorer is zero-shot, *i.e.*, \mathcal{D} is never trained with any generated image or video, and thus, requires no manual annotation effort, unlike prior work [8, 32, 42, 47, 49].

While human detection score is a strong measure, as we show in the experiments, using it as the only reward model will motivate the video generation model to suppress motion, since a static video with good human appearance will give a perfect score, despite not showing the overall motion required in the input text prompt. To this end, we propose an additional action progress score, defined next.

Temporal prompt alignment (P-score) measures the *faithfulness* of the video frames for various action phases. We extract the detailed action phases from the text prompt. For example, the action phases for a lunge can be standing straight with legs apart, bending, holding, and coming back up (*cf.* Fig. 3). Now, given T_i as the text describing the i^{th} phase of the condition, out of a total of N phases, the alignment is defined as

$$\sum_{i=1}^N \text{sim}(\mathbf{V}_{t^i}, T_i) \quad \text{where} \quad t^i = \frac{i * |\mathbf{V}|}{N}$$

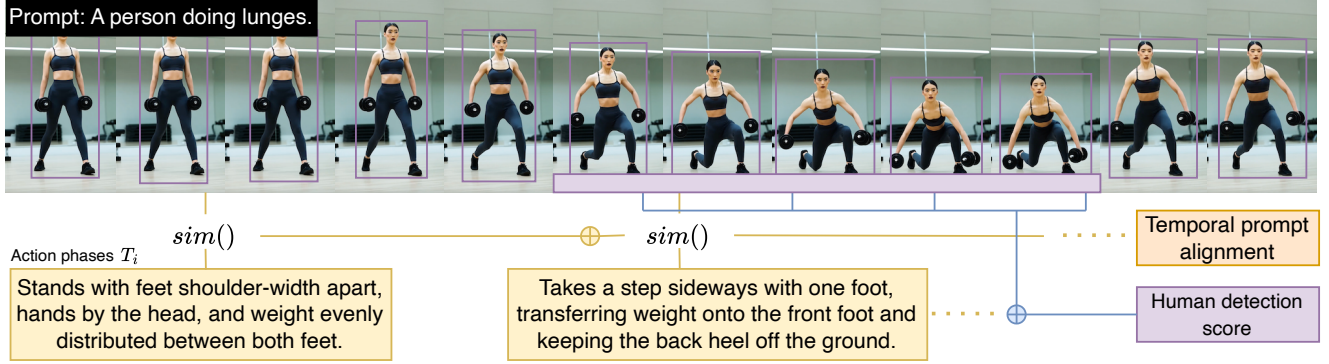


Figure 3. **Our reward model HUDA** quantifies the human detection score and temporal prompt alignment scores. The first term is the confidence level of the human detector in the worst performing window W shown in purple band. Next, temporal prompt alignment score is the average of similarity between phase descriptions T_i and uniformly sampled frames. Overall reward is a weighted average of human detection score and temporal prompt alignment.

where $sim()$ is a similarity measure of visual and text features [23]. This alignment measures action progress by comparing the current frame with the corresponding condition T_i . We represent T_i with text for its interpretability and the ease of generation using off-the-shelf LLMs [2, 7].

The overall reward model HUDA is the sum of human detection score and a weighing factor (α) times the temporal prompt alignment. Fig. 3 shows the reward model calculation for a representative example.

3.3. RL post-training with HUDA

We use the Group Reward Policy Optimization (GRPO) [33, 45] to post-train the video diffusion model to generate outputs with better human appearance. As outlined previously in the Sec. 2, we choose GRPO over DPO for its on-policy training, use of continuous reward, and the ability to use multi-objective reward.

In particular, the objective function for GRPO is

$$\mathcal{J}(\theta) = \mathbb{E}_{\mathbf{V}_i \sim \pi_{\theta_{old}}} \left[\frac{1}{G} \sum_{i=1}^G \min(\mathcal{L}_u, \mathcal{L}_c) \right]$$

where $\mathcal{L}_u = \rho_i A_i$, $\mathcal{L}_c = \text{clip}(\rho_i, 1 - \epsilon, 1 + \epsilon) A_i$
and $\rho_i = \frac{\pi_{\theta}(\mathbf{V}_i | \mathbf{c})}{\pi_{\theta_{old}}(\mathbf{V}_i | \mathbf{c})}$, $A_i = \frac{R(\mathbf{V}_i) - \mu_R}{\sigma_R}$

Here, $\pi_{\theta_{old}}$ and π_{θ} are the policy variants before and after the update, respectively, and \mathbf{V}_i and \mathbf{c} are the video and the conditioning signal, *i.e.*, text prompt. μ_R and σ_R are the mean and standard deviation of the rewards of the G generated samples. \mathcal{L}_u and \mathcal{L}_c are the unclipped and the clipped losses, respectively. Conventional GRPO also has a KL-loss between the original policy and the current policy [26, 33]. However, following [45], we do not use KL-loss since there is no performance gain. This choice also helps save memory since we don't need to keep a copy of the original policy.

3.4. Implementation details

We use ViTDet [24, 43] as the object detector \mathcal{D} . The window size W is 6 frames. We choose $N = 5$ phases, and generate progress descriptions using Llama-3.2 8B [7]. The prompt describes the action as spanning 5 – 7 seconds, and asks for N phase caption, each spanning 1 – 2 seconds. The exact prompt is given in the Appendix C. We use BLIP [23] as the similarity measure $sim()$. Finally, we set the weighing parameter $\alpha = 0.5$ to focus more on human detection score over temporal prompt alignment score.

For video generation training, we experiment with 1.3B and 14B variants of Wan 2.1 [38] for our experiments; the method can be extended to any video diffusion model [12, 21, 35]. We train the model using 32 A100 GPUs for 12 hours. The learning rate for 1.3B and 14B models are 10^{-5} , and 10^{-6} , respectively. During GRPO training, we generate videos with $[H, W, T] = [480, 480, 53]$. We generate 24 videos per prompt, and sample 16 steps using SDE sampler [33, 45]. During inference, we generate videos with $[H, W, T] = [1280, 720, 81]$. We use 50-step sampling with classifier free guidance (CFG) scale 5.0 for both training and testing. These inference parameter choices reflect the best possible setting for the backbone video model [38].

4. Experiments

In this section, we first establish HUDA as the accurate reward model for human appearance and pose. Next, we demonstrate that using HUDA as a reward model in GRPO training improves human appearance in generated videos. To that end, we first discuss the common experimental setup, followed by results. We also discuss ablations, and finally, generalizability of HUDA to improve human-object interactions, and even improved animal video generation.

Method	Accuracy
VLM-as-a-judge [36]	55.0
DanceGRPO [45]	51.5
<hr/>	
VBench-2.0 [49]	72.7
<hr/>	
HUDA (Ours)	77.4

Table 1. **Accuracy** of the various reward models in predicting human-preferred videos. First two rows are zero-shot, and VBench-2.0 is trained for this task. Ours is fully zero-shot and significantly outperforms both zero-shot and trained baselines.

4.1. Experimental Setup

In this section, we discuss experimental setup that is common for both evaluating HUDA as a reward model, and verifying the improvement in video generation.

Creating the training and testing prompt set. We care about human appearance and action, and thus, we create a prompt set to train and test the same. We start with a wide range of activities, representing diverse motions with varying difficulty. Specifically, we leverage a large language model, Llama-3.2-8B [7], to generate 3000 human motion sequences labels. These are categorized into three levels of motion difficulty—easy: standing, walking, clapping; medium: running, jumping, tennis forehand; and hard: backflip, handstand, ski flip. The exact input prompt to generate the motions is given in the Appendix C that describes the diverse range of motion requirements, with examples of easy, medium and difficult motions.

Once we obtain the labels, we use a simple template to convert the labels into full prompts. We use kid, boy, girl, man, and woman as the subject and curate prompts of the format “A {subject} doing {action}”. Finally, we use the prompt expansion in Wan 2.1 [38] to add details to the prompt. We choose a subset of 300 human motion sequences (out of 3000) for evaluation. The evaluation set contains 100 human motions from each difficulty level. The same evaluation split is used for both evaluating HUDA’s performance as a reward model, and showing improved video generation with HUDA.

Baselines. We compare HUDA with the following:

- **VLM-as-a-judge [36]:** Video language models (VLM) are capable of a variety of tasks, showcasing impressive zero-shot performance. In this baseline, we evaluate if zero-shot VLMs can detect abnormal human appearance and motion. Given a video with human, we query the VLM if the video contains any appearance anomaly, prompting it to give yes/no answer. We use the ‘no’ logit probability as the reward score. The exact prompt is given in the Appendix C.
- **VBench-2.0 human anomaly [49]:** VBench-2.0 proposes various video generation benchmarks. In particular, human anomaly detector predicts the likelihood of the video containing anomalous human appearance or motion. The proposed model is trained from samples from

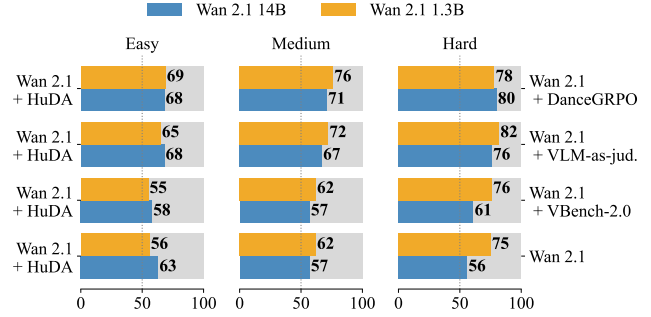


Figure 4. **Video generation win-rate** between HUDA (depicted by colored bars) and previous state-of-the-art baselines (100—HUDA’s win rate). Our method is consistently preferred by human annotators across all settings, with biggest gains in the hard category (avg win-rate 73% vs 63% for easy, across all baselines).

HumanRefiner [8] dataset, along with additional supervision obtained from real and generated videos.

- **Video visual/motion alignment [45]:** Many recent works use VLM-based visual and motion quality scores to improve video. We use DanceGRPO [45] as a representative example to investigate if a combination of visual and motion quality can quantify human appearance.
- **Base model (Wan 2.1) [38]:** This original model is used for evaluating improvements in video generation.

In addition to proposing HUDA, we also explore if other modalities, *e.g.*, 3D/2D pose [44], or optical flow [29] can be used as reward functions. We discuss our early explorations in the Appendix D.

Evaluation setup. Our objective is to experimentally validate HUDA as the correct reward model, and then use HUDA to improve video generation.

Firstly, to evaluate HUDA as a reward model, we collect ground truth annotations from human raters. In accordance to our task, we choose two videos for the same input prompt and ask the annotators to choose the video that has better human appearance. The prompts are from our test set, discussed above. The instructions and examples demonstrate less preferred videos with extra/missing body parts, distorted or implausible poses. We insert test examples to check for the attentiveness of the annotators. We have an annotator quality threshold to ensure correct alignment with human preference. Each sample is annotated by five annotators, and we choose the samples that have four annotators agreeing on an option. A screenshot of the annotation interface is given in the Appendix B.

Secondly, to establish that training with HUDA reward model improves video generation, we compare our outputs with baselines’. Similar to the above, we use the same human annotation setup. Additionally, we also ask the annotators if the generated video is faithful to the text prompt. This additional question is designed to ensure our training did not reduce the prompt faithfulness. Now, we discuss the

A parkour athlete performing a dynamic roll after landing from a jump in a city park.



Wan 2.1 14B



Wan 2.1 14B + HUDA

A martial artist performing a dynamic 540-degree spinning kick in mid-air.

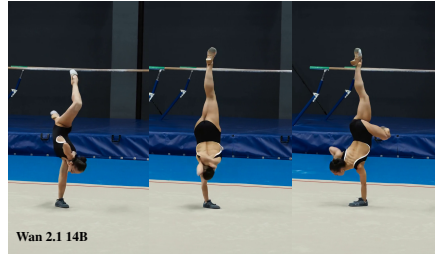


Wan 2.1 14B

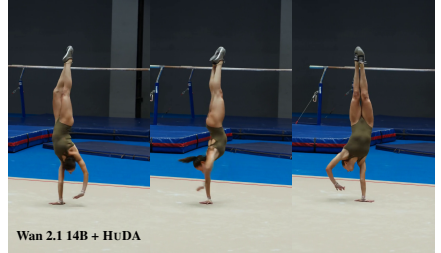


Wan 2.1 14B + HUDA

A gymnast performing a one-arm handstand spin on a gym floor.



Wan 2.1 14B



Wan 2.1 14B + HUDA

Figure 5. **Qualitative comparison** of videos generated by our method (bottom) with Wan 2.1 14B [38] (top). Wan 2.1 generates distorted poses (left), two-headed person (middle), and inconsistent legs (right), whereas Wan 2.1 trained with HUDA generates realistic humans.

specifics of the two evaluations, followed by the results and ablations.

4.2. Evaluating HUDA reward model

Recall that given two videos V_1 and V_2 where V_1 shows better human appearance and motion, a good design of R would imply $R(V_1) > R(V_2)$ for all (V_1, V_2) pairs. Naturally, for a real video V , $R(V)$ should be maximum. Overall, R establishes a way to compare generated videos. Our protocol to evaluate HUDA is described in detail next.

Generating videos with humans. We use Wan 2.1 [38] 1.3B and 14B models, and generate 600 video pairs, i.e., a total of 1200 videos. We use the test set with 300 motion descriptions, as discussed above.

Evaluation metric. As discussed above, we use human annotations to obtain ground truth preferences. We report accuracy as the fraction of samples where HUDA’s relative order matches the preference of annotators’ consensus.

Results. Tab. 1 shows the accuracy for all the methods. We outperform the best zero-shot method (VLM-as-a-judge) by more than 22%. We even outperform VBench-2.0 [49] by more than 3%, even though VBench-2.0 is trained with manually annotated data. Finally, alternate visual/motion quality reward models are not suited for scoring human appearance in generated videos. In summary, our designed HUDA is strongly correlated with the human preferences. We use HUDA to train video diffusion model to generate better humans, as shown next.

4.3. Video generation with HUDA

In this section, we demonstrate utilizing our proposed HUDA to improve video generation. We use GRPO [26, 33,

45], with HUDA as the reward model to *post-train* state-of-the-art video diffusion models.

Training and testing prompt set. We use the same training and testing prompt set, as described in the Sec. 4.1. Specifically for training Wan 2.1 [38] 1.3B, we choose medium and hard motions, whereas, we choose only hard motions for Wan 2.1 [38] 14B. This choice reflects the relative strength of the two variants since GRPO is more efficient with training samples having high variance. Nevertheless, we evaluate on the whole testing set containing an equal split of easy, medium and difficult prompts.

Evaluation metric. In this experiment, we report win-rate between ours and the baseline as the fraction of times the annotator’s preferred video was generated by HUDA.

Results. Fig. 4 shows the results. Our method achieves a better win-rate compared to all the baselines, for all the prompt difficulty levels. Our average win-rate over the baselines is 73% on the hard prompt set, 65% for the medium prompt, and 63% with the easy prompt set. These results showcase the strong improvement in human appearance and motion, using our zero-shot HUDA. Furthermore, the prompt faithfulness win-rate over the base Wan 2.1 is within $\pm 4\%$, implying that our training preserves the prompt faithfulness; detailed faithfulness result is in the Appendix D. Overall, we significantly improve human appearance, while preserving prompt faithfulness.

Visualizations. Fig. 5 shows representative outputs from the GRPO training, and compares them with the base model (also see the Appendix A for video outputs). We see many anomalies in the base model that are absent in our generations. For example, a video of martial art 540-spinning kick shows two heads, whereas our generation correctly shows

Reward model	Accuracy	Reward model	HuDA Win-rate
GroundingDINO [4]	71.2	HuDA vs	
Only P-score	59.1	Only H-score	75.0
Only H-score	74.2	Prompt-video sim.	57.0
Prompt-video sim.	75.5	Optical flow [29]	90.0
Optical flow [29]	74.8	Method	HuDA score
Fewer frames (R)	71.8	Ours w/ KL-div	0.961
Fewer frames (F)	71.2	Ours w/o prompt exp.	0.936
HuDA	77.4	Ours	0.975

Table 2. **Ablations.** On left, we compare HuDA to alternative reward functions described in Sec. 4.4.1 using accuracy measure from Sec. 4.2. On right (top), we compare generation performance with variants of HuDA as the reward model using win-rate. On right (bottom), we evaluate different training settings and the reward obtained on a validation set.

the action without any human appearance anomaly. We see the same improvement for all motion difficulty levels.

4.4. Ablations

In this section, we present ablations to assess the contribution of each component and to show that our approach remains effective across varied design and training choices. Each of the aspects are discussed next.

4.4.1. HuDA ablations

We compare HuDA with the following:

- Open-world object detector \mathcal{D} : We replace the closed-vocabulary ViTDet [24, 43] with an open vocabulary GroundingDINO [4, 28] to evaluate if we can use class-independent open world object detector. We try various open world terms: ‘person’, ‘human’, ‘eyes’, ‘legs’, ‘hands’, and a combination of these terms. We report the best performing combination.
- Only temporal prompt alignment score (Only P-score): In this ablation, we only use P-score as the reward model and do not use human detection score (H-score).
- Only human detection score (Only H-score): We investigate the role of P-score by removing it for this ablation.
- Prompt-video similarity as P-score: In this ablation, we replace our P-score with the average similarity score between the prompt and all the video frames. We use the same BLIP [23] for similarity calculation.
- Optical flow as P-score: In this ablation, we explore if optical flow [29] can serve as P-score, instead of a language-based similarity measure.
- Using fewer frames: In this ablation, we evaluate the reward on a subset of frames. Specifically, we explore two variants: randomly sampled ordered subset of 20% frames (R), and a subset having the first 20% frames (F).

Results. Tab. 2 (left) shows the results. We report accuracy, as defined in the Sec. 4.2. HuDA’s accuracy outperforms all the other choices. In particular, despite the flexibility of open-world object detector, a closed vocabulary class-based

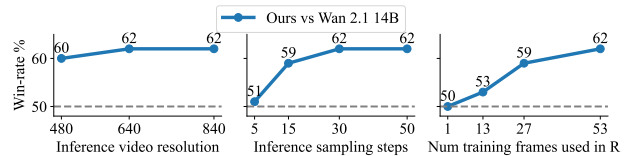


Figure 6. **Ablating design-choices in HuDA:** inference video resolution (left), number of sampling steps (middle), and number of frames used to compute HuDA during training (right). We use human evaluation win-rate against the base video model. We find our gain is consistent across resolutions and increases marginally with inference sampling steps. Our performance significantly increases with more frames considered.

object segmentation gives stronger performance. Next, using only P-score gives very low performance since action progress calculation is uncorrelated with human appearance quality. Conversely, if we only use human detection score, the human appearance is very good but the motion is very conservative and often unfaithful to the input prompt. Next, prompt-video similarity can be high even with very little motion since overall prompt does not have sub-action descriptions. Moreover, optical flow also performs worse than HuDA due to the inability of optical flow to attend to human motion specifically. Lastly, using fewer frames degrades the performance significantly, verifying no single-frame bias and no over-reliance on the first few frames.

4.4.2. Ablations of video generation with HuDA

We experiment with various choices in video generation post-training. We use the high-performing subset of reward models from the ablations above, and train GRPO using those reward models to further establish failures of those model choices. All the experiments are done with Wan 2.1 14B on the easy prompt set. Specifically, we perform the following ablations, already described above: Only human detection score (only H-score), prompt-video similarity as P-score, and finally, optical flow as P-score. Tab. 2 (top right) shows the win-rate for the chosen ablations. We observe that HuDA is a better reward model than these ablations. Specifically, both human detection score (H-score) and temporal prompt alignment score (P-score) are crucial for improving humans in generated videos.

Next, we ablate our choices in the GRPO training setup. We investigate the affect of using KL-divergence in the GRPO training, and that of not using prompt expansion. Tab. 2 (bottom right) shows the performance. We simply use the reward score, *i.e.*, HuDA to evaluate the performance since the reward model is the same in all the methods being compared. We observe that KL-divergence is not very helpful in the performance, while requiring more memory since we need to maintain a copy of the original policy. Moreover, we do not see an improvement in GRPO training without prompt expansion.

A playful monkey jumping on a grassy field.

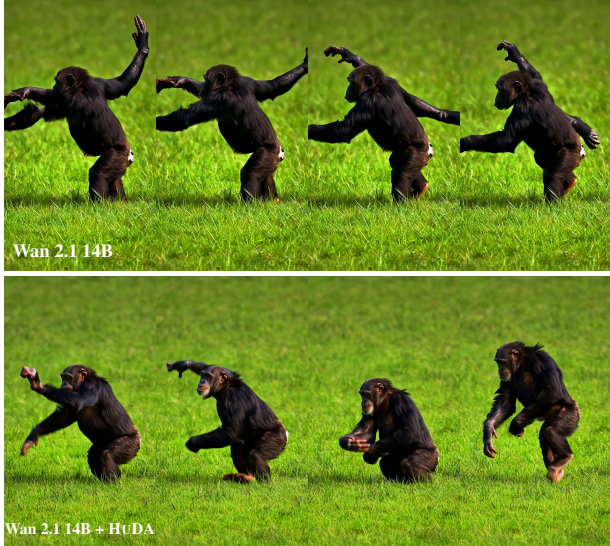


Figure 7. **Model trained with HUDA generates better zero-shot animal videos**, whereas the base model generates videos with extra/missing body parts and unrealistic poses, showing that HUDA enables the model to generate realistic body deformations.

Lastly, we present our results with various video parameters to showcase that our performance gain is agnostic to those model choices:

- Impact of inference video resolution: During inference, we generate videos with different resolutions to show that the improved performance is independent of the resolution. We consider an aspect ratio of 1.
- Impact of the number of inference steps: We generate videos with varying numbers of steps to show that the performance gain is consistent across different step counts.
- Impact of the number of training frames considered: We investigate if all frames are required when calculating HUDA. In place of 53 training frames, we consider 1, 13, or 27 frames during training.

Fig. 6 shows ablation plots for various training and inference choices. We observe that our gain is significant for all video sizes, for all reasonable number of sampling steps. Finally, an increasing win-rate when more frames are considered signals no single-frame bias in HUDA.

4.5. Beyond human video generation

While HUDA is designed for optimizing human video generation, we find the benefits with HUDA extend beyond that. In particular, we find that a model trained with HUDA even improves generation of animals, and human-object interactions. We discuss these next.

Generating videos with animals. We observe that the deformations in humans are similar to those in animals such as dogs, cats, and monkeys. Although HUDA is not specifically designed for animal detection, videos generated by

Detector \mathcal{D}

A professional tennis player executing a powerful swing.



Figure 8. **Example of improvement in human-object interaction.** Reward from our HUDA is higher when human-object interactions are correct (left). Training video generation with HUDA improves human-object interaction in generated videos (right).

our trained model exhibit the correct animal motions.

We use Llama-3.2 8B [7] to create a prompt set for this experiment. We use dog, cat, chimpanzee, monkey, ape, gorilla, and orangutan as the subject and prompt the language model to generate 100 prompts that shows various actions like backflip, jump, cartwheel, etc. Specifically, actions that are not typical characteristics of these animals are also included to test the generation ability. Fig. 7 illustrates one such case. The base model outputs a monkey with three hands, while our method produces the correct anatomy. More examples in the Appendix A.

Improved human-object interaction. Improving human appearance also improves human-object interactions since the two are tied together in natural videos. We observe that the human detection score from \mathcal{D} is low in videos with poor human-object interactions, because of worse human hand and/or body appearance. For example, in Fig. 8 (left), we see a lower detection score when the tennis racket and hand is distorted, as opposed to when they are correctly generated. Consequently, we find that our model trained with HUDA has a nice side-effect of even generating better human-object interactions compared to the baseline model. Fig. 8 (right) shows one such example in tennis, more examples in the Appendix A. In summary, the advantages of HUDA goes beyond improvement in human appearance.

5. Conclusion

In this work, we propose HUDA, a remarkably simple reward model that can correctly quantify the human appearance, motion, and action progress. We first show that this reward model correlates well with human preference. Our zero-shot method’s gain far exceeds other zero-shot meth-

ods, and even outperforms models trained with manually annotated data. Next, we use the proposed reward model HUDA to improve video generation with GRPO. As observed from the human preference studies, videos generated by our method is preferred by human raters over all other competing baselines. Lastly, we show that our training helps the model better understand deformable objects, thus generalizing the improvements to human-object interactions and animal video generation.

References

- [1] Jie An, Songyang Zhang, Harry Yang, Sonal Gupta, Jia-Bin Huang, Jiebo Luo, and Xi Yin. Latent-shift: Latent diffusion with temporal shift for efficient text-to-video generation. *arXiv preprint arXiv:2304.08477*, 2023. 2
- [2] Jinze Bai, Shuai Bai, Yunfei Chu, Zeyu Cui, Kai Dang, Xiaodong Deng, Yang Fan, Wenbin Ge, Yu Han, Fei Huang, et al. Qwen technical report. *arXiv preprint arXiv:2309.16609*, 2023. 4
- [3] Andreas Blattmann, Robin Rombach, Huan Ling, Tim Dockhorn, Seung Wook Kim, Sanja Fidler, and Karsten Kreis. Align your latents: High-resolution video synthesis with latent diffusion models. In *Proceedings of the IEEE/CVF conference on computer vision and pattern recognition*, 2023. 2
- [4] Kai Chen, Jiaqi Wang, Jiangmiao Pang, Yuhang Cao, Yu Xiong, Xiaoxiao Li, Shuyang Sun, Wansen Feng, Ziwei Liu, Jiarui Xu, Zheng Zhang, Dazhi Cheng, Chenchen Zhu, Tianheng Cheng, Qijie Zhao, Buyu Li, Xin Lu, Rui Zhu, Yue Wu, Jifeng Dai, Jingdong Wang, Jianping Shi, Wanli Ouyang, Chen Change Loy, and Dahua Lin. MMDetection: Open mmlab detection toolbox and benchmark. *arXiv preprint arXiv:1906.07155*, 2019. 7
- [5] Florinel-Alin Croitoru, Vlad Hondru, Radu Tudor Ionescu, Nicu Sebe, and Mubarak Shah. Curriculum direct preference optimization for diffusion and consistency models. In *Proceedings of the Computer Vision and Pattern Recognition Conference*, 2025. 3
- [6] Emily Denton and Rob Fergus. Stochastic video generation with a learned prior. In *International conference on machine learning*, pages 1174–1183. PMLR, 2018. 2
- [7] Abhimanyu Dubey, Abhinav Jauhri, Abhinav Pandey, Abhishek Kadian, Ahmad Al-Dahle, Aiesha Letman, Akhil Mathur, Alan Schelten, Amy Yang, Angela Fan, et al. The llama 3 herd of models. *arXiv e-prints*, 2024. 4, 5, 8
- [8] Guian Fang, Wenbiao Yan, Yuanfan Guo, Jianhua Han, Zutaotao Jiang, Hang Xu, Shengcai Liao, and Xiaodan Liang. Humanrefiner: Benchmarking abnormal human generation and refining with coarse-to-fine pose-reversible guidance. In *ECCV*, 2024. 2, 3, 5
- [9] Daniel Geng, Max Hamilton, and Andrew Owens. Comparing correspondences: Video prediction with correspondence-wise losses. In *Proceedings of the IEEE/CVF Conference on Computer Vision and Pattern Recognition*, pages 3365–3376, 2022. 2
- [10] Ross Girshick. Fast r-cnn. In *Proceedings of the IEEE international conference on computer vision*, 2015. 3
- [11] Yuwei Guo, Ceyuan Yang, Anyi Rao, Zhengyang Liang, Yaohui Wang, Yu Qiao, Maneesh Agrawala, Dahua Lin, and Bo Dai. Animatediff: Animate your personalized text-to-image diffusion models without specific tuning. *arXiv preprint arXiv:2307.04725*, 2023. 2
- [12] Yoav HaCohen, Nisan Chiprut, Benny Brazowski, Daniel Shalem, Dudu Moshe, Eitan Richardson, Eran Levin, Guy Shiran, Nir Zabari, Ori Gordon, et al. Ltx-video: Realtime video latent diffusion. *arXiv preprint arXiv:2501.00103*, 2024. 2, 4
- [13] Ligong Han, Jian Ren, Hsin-Ying Lee, Francesco Barbieri, Kyle Olszewski, Shervin Minaee, Dimitris Metaxas, and Sergey Tulyakov. Show me what and tell me how: Video synthesis via multimodal conditioning. In *Proceedings of the IEEE/CVF Conference on Computer Vision and Pattern Recognition*, pages 3615–3625, 2022. 2
- [14] Kaiming He, Georgia Gkioxari, Piotr Dollár, and Ross Girshick. Mask r-cnn. In *Proceedings of the IEEE international conference on computer vision*, 2017. 3
- [15] Yingqing He, Tianyu Yang, Yong Zhang, Ying Shan, and Qifeng Chen. Latent video diffusion models for high-fidelity long video generation. *arXiv preprint arXiv:2211.13221*, 2022. 2
- [16] Jonathan Ho, William Chan, Chitwan Saharia, Jay Whang, Ruiqi Gao, Alexey Gritsenko, Diederik P Kingma, Ben Poole, Mohammad Norouzi, David J Fleet, et al. Imagen video: High definition video generation with diffusion models. *arXiv preprint arXiv:2210.02303*, 2022.
- [17] Jonathan Ho, Tim Salimans, Alexey Gritsenko, William Chan, Mohammad Norouzi, and David J. Fleet. Video diffusion models. 2022.
- [18] Wenyi Hong, Ming Ding, Wendi Zheng, Xinghan Liu, and Jie Tang. Cogvideo: Large-scale pretraining for text-to-video generation via transformers. *arXiv preprint arXiv:2205.15868*, 2022. 2
- [19] Beibei Jin, Yu Hu, Qiankun Tang, Jingyu Niu, Zhiping Shi, Yinhe Han, and Xiaowei Li. Exploring spatial-temporal multi-frequency analysis for high-fidelity and temporal-consistency video prediction. In *Proceedings of the IEEE/CVF conference on computer vision and pattern recognition*, 2020. 2
- [20] Levon Khachatryan, Andranik Movsisyan, Vahram Tadevosyan, Roberto Henschel, Zhangyang Wang, Shant Navasardyan, and Humphrey Shi. Text2video-zero: Text-to-image diffusion models are zero-shot video generators. In *Proceedings of the IEEE/CVF International Conference on Computer Vision*, 2023. 2
- [21] Weijie Kong, Qi Tian, Zijian Zhang, Rox Min, Zuozhuo Dai, Jin Zhou, Jiangfeng Xiong, Xin Li, Bo Wu, Jianwei Zhang, et al. Hunyuanvideo: A systematic framework for large video generative models. *arXiv preprint arXiv:2412.03603*, 2024. 2, 4
- [22] Manoj Kumar, Mohammad Babaeizadeh, Dumitru Erhan, Chelsea Finn, Sergey Levine, Laurent Dinh, and Durk Kingma. Videoflow: A conditional flow-based model for stochastic video generation. *arXiv preprint arXiv:1903.01434*, 2019. 2

- [23] Junnan Li, Dongxu Li, Caiming Xiong, and Steven Hoi. Blip: Bootstrapping language-image pre-training for unified vision-language understanding and generation. In *International conference on machine learning*, 2022. 4, 7
- [24] Yanghao Li, Hanzi Mao, Ross Girshick, and Kaiming He. Exploring plain vision transformer backbones for object detection. In *European conference on computer vision*, pages 280–296. Springer, 2022. 1, 3, 4, 7
- [25] Tsung-Yi Lin, Michael Maire, Serge Belongie, James Hays, Pietro Perona, Deva Ramanan, Piotr Dollár, and C Lawrence Zitnick. Microsoft coco: Common objects in context. In *European conference on computer vision*, pages 740–755. Springer, 2014. 3
- [26] Jie Liu, Gongye Liu, Jiajun Liang, Yangguang Li, Jiaheng Liu, Xintao Wang, Pengfei Wan, Di Zhang, and Wanli Ouyang. Flow-grpo: Training flow matching models via online rl. *arXiv preprint arXiv:2505.05470*, 2025. 2, 3, 4, 6
- [27] Runtao Liu, Haoyu Wu, Ziqiang Zheng, Chen Wei, Yingqing He, Renjie Pi, and Qifeng Chen. Videodpo: Omni-preference alignment for video diffusion generation. In *Proceedings of the Computer Vision and Pattern Recognition Conference*, 2025. 2, 3
- [28] Shilong Liu, Zhaoyang Zeng, Tianhe Ren, Feng Li, Hao Zhang, Jie Yang, Chunyuan Li, Jianwei Yang, Hang Su, Jun Zhu, et al. Grounding dino: Marrying dino with grounded pre-training for open-set object detection. *arXiv preprint arXiv:2303.05499*, 2023. 7
- [29] Henrique Morimitsu, Xiaobin Zhu, Roberto M Cesar, Xiangyang Ji, and Xu-Cheng Yin. Dpflow: Adaptive optical flow estimation with a dual-pyramid framework. In *Proceedings of the Computer Vision and Pattern Recognition Conference*, 2025. 5, 7, 3
- [30] Sanghyeon Na, Yonggyu Kim, and Hyunjoon Lee. Boost your human image generation model via direct preference optimization. In *Proceedings of the Computer Vision and Pattern Recognition Conference*, 2025. 3
- [31] Wenkang Shan, Zhenhua Liu, Xinfeng Zhang, Zhao Wang, Kai Han, Shanshe Wang, Siwei Ma, and Wen Gao. Diffusion-based 3d human pose estimation with multi-hypothesis aggregation. In *Proceedings of the IEEE/CVF International Conference on Computer Vision (ICCV)*, pages 14761–14771, 2023. 3
- [32] Dian Shao, Mingfei Shi, Shengda Xu, Haodong Chen, Yongle Huang, and Binglu Wang. Finephys: Fine-grained human action generation by explicitly incorporating physical laws for effective skeletal guidance. In *CVPR*, 2025. 2, 3
- [33] Zhihong Shao, Peiyi Wang, Qihao Zhu, Runxin Xu, Junxiao Song, Xiao Bi, Haowei Zhang, Mingchuan Zhang, YK Li, Yang Wu, et al. Deepseekmath: Pushing the limits of mathematical reasoning in open language models. *arXiv preprint arXiv:2402.03300*, 2024. 4, 6
- [34] Uriel Singer, Adam Polyak, Thomas Hayes, Xi Yin, Jie An, Songyang Zhang, Qiyuan Hu, Harry Yang, Oron Ashual, Oran Gafni, et al. Make-a-video: Text-to-video generation without text-video data. *arXiv preprint arXiv:2209.14792*, 2022. 2
- [35] Genmo Team. Mochi 1. <https://github.com/genmoai/models>, 2024. 4
- [36] Qwen Team. Qwen2.5: A party of foundation models, 2024. 2, 5, 3
- [37] Bram Wallace, Meihua Dang, Rafael Rafailov, Linqi Zhou, Aaron Lou, Senthil Purushwalkam, Stefano Ermon, Caiming Xiong, Shafiq Joty, and Nikhil Naik. Diffusion model alignment using direct preference optimization. In *CVPR*, 2024. 2, 3
- [38] Team Wan, Ang Wang, Baole Ai, Bin Wen, Chaojie Mao, Chen-Wei Xie, Di Chen, Fei Wu Yu, Haiming Zhao, Jianxiao Yang, et al. Wan: Open and advanced large-scale video generative models. *arXiv preprint arXiv:2503.20314*, 2025. 2, 4, 5, 6, 3
- [39] Boyuan Wang, Xiaofeng Wang, Chaojun Ni, Guosheng Zhao, Zhiqin Yang, Zheng Zhu, Muyang Zhang, Yukun Zhou, Xinze Chen, Guan Huang, et al. Humandreamer: Generating controllable human-motion videos via decoupled generation. In *CVPR*, 2025. 2, 3
- [40] Jiuniu Wang, Hangjie Yuan, Dayou Chen, Yingya Zhang, Xiang Wang, and Shiwei Zhang. Modelscope text-to-video technical report. *arXiv preprint arXiv:2308.06571*, 2023. 2
- [41] Yaohui Wang, Piotr Bilinski, Francois Bremond, and Antitza Dantcheva. Imaginator: Conditional spatio-temporal gan for video generation. In *Proceedings of the IEEE/CVF winter conference on applications of computer vision*, pages 1160–1169, 2020. 2
- [42] Zeqing Wang, Qingyang Ma, Wentao Wan, Haojie Li, Keze Wang, and Yonghong Tian. Is this generated person existed in real-world? fine-grained detecting and calibrating abnormal human-body. In *CVPR*, 2025. 2, 3
- [43] Yuxin Wu, Alexander Kirillov, Francisco Massa, Wan-Yen Lo, and Ross Girshick. Detectron2. <https://github.com/facebookresearch/detectron2>, 2019. 4, 7, 3
- [44] Yufei Xu, Jing Zhang, Qiming Zhang, and Dacheng Tao. Vitpose: Simple vision transformer baselines for human pose estimation. *Advances in neural information processing systems*, 2022. 5, 3
- [45] Zeyue Xue, Jie Wu, Yu Gao, Fangyuan Kong, Lingting Zhu, Mengzhao Chen, Zhiheng Liu, Wei Liu, Qiushan Guo, Weilin Huang, et al. Dancegrpo: Unleashing grpo on visual generation. *arXiv preprint arXiv:2505.07818*, 2025. 2, 3, 4, 5, 6
- [46] Shohei Yamamoto, Antonio Tejero-de Pablos, Yoshitaka Ushiku, and Tatsuya Harada. Conditional video generation using action-appearance captions. *arXiv preprint arXiv:1812.01261*, 2018. 2
- [47] Fan Yang, Ru Zhen, Jianing Wang, Yanhao Zhang, Haoxiang Chen, Haonan Lu, Sicheng Zhao, and Guiguang Ding. Heie: Mllm-based hierarchical explainable aigc image implausibility evaluator. In *CVPR*, 2025. 2, 3
- [48] Zhuoyi Yang, Jiayan Teng, Wendi Zheng, Ming Ding, Shiyu Huang, Jiazheng Xu, Yuanming Yang, Wenyi Hong, Xiaohan Zhang, Guanyu Feng, et al. Cogvideox: Text-to-video diffusion models with an expert transformer. *arXiv preprint arXiv:2408.06072*, 2024. 2
- [49] Dian Zheng, Ziqi Huang, Hongbo Liu, Kai Zou, Yanan He, Fan Zhang, Lulu Gu, Yuanhan Zhang, Jingwen He, Wei-Shi Zheng, et al. Vbench-2.0: Advancing video generation

benchmark suite for intrinsic faithfulness. *arXiv preprint*
arXiv:2503.21755, 2025. [2](#), [3](#), [5](#), [6](#)

Human detectors are surprisingly powerful reward models

Supplementary Material

A. Videos for all figures in the main paper

We attach an HTML webpage ‘videos.html’ that contains qualitative results, including videos for the figures in the main paper.

B. Human evaluation Setup

Fig. 9 shows the instructions provided to the human annotators. We first show good and bad examples of various aspects of human appearance and motion. We focus on extra or missing body parts, pose sequence and movements, and physics. Next, we show an example of good and bad prompt faithfulness. These examples are visible to the annotators at all times, for their quick reference.

Next, Fig. 10 shows the annotation questions. We first ask whether one, both, or neither of the videos are faithful to the prompt. This question helps us assess whether the generated videos are meaningful. We do not want improvements in human appearance to come at the expense of prompt faithfulness. The second question asks which video has the better human appearance. Unlike the first question, we do not include a neutral option, since even when the differences are minimal, we want annotators to choose the video with better human appearance.

C. LLM prompts

The following snippet contains the LLM prompt to generate 3000 human motion sequence labels, as discussed in Sec. 4.1. To ensure the response length does not exceed the maximum new tokens limit, we ask the LLM to generate motion sequences for each difficulty level separately, *i.e.*, 1000 output motions per response.

Generate a list of 3000 human movement concepts and categorize them into three difficulty levels based on how physically challenging, dynamic, and coordinated the movement is.

Use the following structure:

- easy (1000 items): simple motions like sitting, walking, waving
- medium (1000 items): moderately dynamic motions like running, jumping, crawling, kicking
- hard (1000 items): acrobatic, athletic, or highly complex movements like flips, vaults, breakdancing moves

How to evaluate correctness of human appearance and text alignment? -- aspects to consider
When selecting which video aligns better with the text prompt, please pay attention to the following factors.

Aspect	Explanation	Good Example	Poor Example
Human appearance and motion correctness	There should not be any extra or missing body parts, e.g., extra legs, missing hands.	The video shows correct body parts without any extra or missing body part. (good human appearance).	The video shows the person having three legs at once (missing or extra body parts).
		Shows correct body pose -- legs can move sideways (good body pose)	Knees cannot fold inwards (implausible body pose)
Physics should be correct, e.g., jump, turns.	The body pose and movement should be plausible.	The twisting motion is correct, and no turn is implausible. (good physics and motions; ignore bad physics and motions of the ball)	Too much motion and fast swirl that's not possible. (bad physics and motions)
		prompt: A person doing squats. The cat is moving its paw to play the piano. (good motion / temporal faithfulness)	prompt: A person doing backflip. The human is correct but no backflip is visible/shown. (bad motion / temporal faithfulness)
Prompt Text Motion / Temporal Faithfulness	The motion of the human should match the text prompt description.		

Figure 9. Annotation interface instructions. We describe the various axes of judging human appearance and motion, and provide good and bad examples for each of them.

Requirements:

- Focus ONLY on human actions that require a full-body view (no micro-actions like winking, blinking, finger tapping, eye movement, typing fingers, etc.).
- Return the result as valid JSON, exactly in the format:

```
{  
  "easy": ["concept1", ...],  
  "medium": ["concept1", ...],  
}
```

PLEASE ANSWER BOTH QUESTIONS BELOW.

The submit button is disabled for the first ten seconds of each assignment. Please answer both questions and watch both videos!

Watch the following two pieces of video and select the one that you think has better **HUMAN APPEARANCE AND MOTION** and better alignment with the **text prompt** according to the 2 factors (spatial text faithfulness, motion / temporal text faithfulness):

Text: A runner sprinting on grass

Video 1:



Video 2:



Question 1. - Which video shows better alignment with the text prompt, including motion and temporal consistency?

Video 1 Video 2 None of them Both of them

Question 2. - Which video shows better human pose and realistic motions?

Video 1 Video 2

Figure 10. **Annotation questions.** We provide the two videos being compared, and the text prompt, and ask the annotators two questions. The first question asks if one, both, or none of the videos are faithful to the input prompt. The second question asks which of the two videos shows more realistic human appearance.

```
“hard”: [{"concept1", ...}]
```

- Avoid duplicates strictly across all categories.
- Ensure the list is highly diverse across daily actions, sports, athletics, dance, martial arts, gymnastics, acrobatics, parkour, yoga, pilates, diving, circus arts, rehabilitation movements, etc.
- Concepts should be names only (no descriptions).
- Generate the sets one category at a time.
- Start now by generating the 1000 concepts for the hard category only.

Next, the following snippet contains the LLM prompt to generate action phases T_i given a text prompt, as discussed in Sec. 3:

You are an expert video coach and scriptwriter. Given a high-level caption for a video-generation prompt, break it into exactly 5 temporally ordered, visually concrete micro-phases that together span 5 seconds total around the core action (NOT much longer than that).

STRICT TEMPORAL SCOPE:

- Model exactly a 5 second window centered on the core action.

- Each phase should represent 0.5-1.5 seconds (max 2 seconds).
- Do NOT include pre-roll/setup (e.g., “walks into the court”, “approaches the plate”) or post-roll (e.g., “leaves the scene”).
- Start at the moment the action preparation begins (e.g., split-step or load) and end right after follow-through/recovery.

VISUAL CONCRETENESS:

- Phases must be camera-visible body/object states and motions (stance, weight shift, unit turn, racquet/arm path, contact, follow-through), not narrative fluff.
- 1-2 sentences per phase, present tense, specific nouns/verbs, no questions.
- Maintain tight temporal continuity and causal flow across phases.
- If the caption is ambiguous, choose a plausible concrete interpretation centered on the core action in 5 seconds.

FORMAT (JSON only, no markdown or extra text):

```
{
  "caption": "{original caption}",
  "phases": [
    "id": 1, "name": "{short micro-phase label}",
    "description": "< 1-2 sentences, ≤ 2s of actioni",
    "id": 2, "name": "...", "description": "...",
    "id": 3, "name": "...", "description": "...",
    "id": 4, "name": "...", "description": "...",
    "id": 5, "name": "...", "description": "..."
  ]
}
```

NEGATIVE EXAMPLES (DO NOT DO):

- “The player walks into the court...” (too early; out of 5s window)
- “He celebrates and exits the frame.” (post-roll; out of 5s window)
- Vague phrases like “then he moves” without body mechanics.

QUALITY TARGET (for something like “Rafael Nadal plays a forehand”):

- Phase 1 could be split-step + unit turn/load,
- Phase 2 racquet take-back + hip/shoulder coil,
- Phase 3 step/weight transfer + swing initiation,
- Phase 4 contact + extension,
- Phase 5 follow-through + balanced recovery.

Finally, the following snippet contains the LLM prompt for the VLM-as-a-judge baseline, as introduced in Sec. 4.1.

Method	Accuracy
VLM-as-a-judge [36]	55.0
DanceGRPO [45]	51.5
VBench-2.0 [49]	72.7
2D pose [44]	62.3
3D pose [31]	63.4
Optical flow [29]	60.2
HUDA (Ours)	77.4

Table 3. **Accuracy** of additional reward models (gray rows) in predicting human-preferred videos. Our HUDA, using human detection confidence, outperforms models using alternate modalities, *i.e.*, 2D/3D pose, and optical flow.

We ask 4 questions, and take the score as the worst ‘no’ logit probability, since the human appearance is as good as the worst aspect.

The video lasts for “{time of the video}” seconds, and “{number of frames}” frames are uniformly sampled from it. These frames are located at “{frame timesteps}”. Return yes or no only for the following questions:

- Q1. Across the entire video, does the person’s pose sequence remain realistic without unnatural twists or left-right flips?
- Q2. Are all body parts present or absent in ways that look natural, with no unnatural extra or missing parts beyond normal occlusion or clipping?
- Q3. Do all body parts remain clearly distinct from the background throughout the video, without dissolving or fading away, even if they clip or go out of frame?
- Q4. Does the video show realistic physics and natural human-object interactions?

D. Additional Results and Ablations

D.1. Additional HUDA comparisons

In this section, we show results with additional reward models, as part of our early explorations in this direction. We explore the following reward models:

- 2D pose [44]: In this baseline, we employ a video to 2D pose method [44] in inference mode, and obtain 2D pose sequences for real and generated videos. The real videos are obtained from the COCO [25] dataset, and the generated videos are obtained from our prompt set, with Wan 2.1 [38] 1.3B and 14B. The output poses are used to train a transformer model to output a class label, with CLS token used as the aggregate representation.
- 3D pose [31]: This baseline is similar to the above 2D pose baseline, except we use inferred 3D poses as input to the transformer architecture.

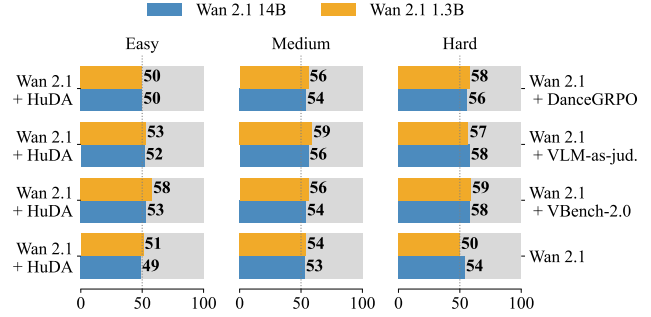


Figure 11. **Prompt faithfulness win-rates.** Prompt faithfulness comparison between baselines and our model trained with HUDA as the reward model. Despite HUDA’s focus on improving human appearance, the prompt faithfulness win-rate remains within 47–54%, showing that prompt faithfulness is preserved. In particular, the temporal prompt alignment module (Sec. 3) in HUDA helps maintain faithfulness.

- Optical flow [29]: We extract optical flow from real and generated videos. The videos are the same as discussed in the 2D pose baseline.

Tab. 3 shows the results. We see that attempting this task in an alternate modality, *i.e.*, pose or flow, is not beneficial. The key issue is that the transformation from the pixel space to the pose or the flow space assumes correct human appearance, since all the models trained for these tasks use only real videos. Therefore, unlike pixel-space, where we see the effectiveness of human detector [24, 43] in zero-shot setting, pose and flow modalities are not appropriate reward models for this task.

D.2. Faithfulness of videos generated with HUDA

In addition to ensuring an improvement in human appearance, we compare the prompt faithfulness between videos generated with HUDA and the baselines. Comparing faithfulness is crucial since any improvement in human appearance is not helpful if the prompt faithfulness decreases. For example, generating a static person will always give a high human appearance score. However, such a scenario is undesirable. At the same time, our focus is on improving human appearance. Therefore, we want the prompt faithfulness to be as good as the model without training with HUDA, while significantly increasing the human appearance win-rate.

Fig. 11 shows the results. We observe that compared to Wan 2.1 [38], the same model trained with HUDA has a prompt faithfulness win-rate between 48% to 54% across the three testing splits (easy, medium, and hard). Other reward models, *i.e.*, Wan 2.1 + VLM-as-a-judge and VBench-2.0 [49] do not use temporal prompt alignment score, and hence, our prompt faithfulness win-rate with them is higher.

Detector \mathcal{D} scores.



Figure 12. **Capturing fast changes of direction is challenging.** The crossing of legs changes rapidly within a few frames, indicating implausible motion. Both frames show correct pose, and hence, HUDA does not capture this motion implausibility. We observe that all reward models fail for this case.

E. Limitation

While HUDA improves human appearance across diverse settings, we observe some instances where the output score from HUDA is high for videos with imperfect human appearance. In particular, since human detection score aggregates frame-level scores, human appearance inconsistency during fast movements is not captured by HUDA. Fig. 12 shows one such example. The crossing of legs changes within a few frames, indicating implausibility. Each individual frame by itself is correct. Hence, HUDA incorrectly scores this video high. The same limitation is observed in all the reward models we compare against. However, we observe very few cases of this type of implausibility.